

## Brittle-Ductile Transition in Reactive PBT/SAN Blends

Saisamorn Lumlong, Keiichi Kuboyama, Tsuneo Chiba, Toshiaki Ougizawa\*

**Summary:** Toughening of reactive poly(butylene terephthalate) (PBT)/styrene-acrylonitrile copolymer (SAN) blends was studied. PBT/SAN with glycidyl methacrylate (SAN-GMA) (70/30) behaved in ductile manner on tensile test, while PBT/SAN (70/30) blend failed in brittle manner. Additionally, poly[methylene (phenylene isocyanate)] (PMPI) was added to the PBT/SAN-GMA blend, where it was expected that PMPI would assist the reaction between PBT and SAN-GMA, and then the strain at break was improved. PBT/SAN/PMPI (70/30/4) also behaved in ductile manner, although the interfacial adhesion strength between matrix and dispersed phase was extremely weaker than that in PBT/SAN-GMA blend. From the results, it was found that PMPI acted as a compatibilizer without copolymer formation at the interface and then PBT/SAN behaved in ductile manner in higher SAN content by PMPI effect.

**Keywords:** blends; brittle-ductile transition; PBT; PMPI; SAN

### Introduction

Poly(butylene terephthalate) (PBT) is well known as an excellent engineering thermoplastic which has good abrasion resistance, electric insulation, solvent resistance, heat resistance and so on. Though it also has high Izod impact strength under unnotched condition, notched PBT specimen fails in brittle manner. This disadvantage can be improved by blending with acrylonitrile-butadiene-styrene (ABS) resin.<sup>[1]</sup> However, the improvement of toughness was observed within a limited condition, that is, blend composition, mixing temperature, shear rate, viscosity ratio of polymers and so on, because PBT and ABS are immiscible. ABS domains can coalesce during melt-mixing process at the certain low shear condition resulting in a reduction in mechanical properties.<sup>[2]</sup>

Generally, to get finer morphology and to strengthen interfacial adhesion between matrix and dispersed phases in an immiscible blend, suitable block or graft copolymers are added to the blend as a compatibilizer. In the industrial use, reactive processing is preferred, that is, addition of functionalized polymer, which is miscible with one blend component and reactive toward the other one, leads to the *in situ*-formed graft copolymer. The copolymer tends to stay at the interface, and thus acts as an effective compatibilizer between two immiscible polymers.<sup>[3–6]</sup>

In the case of blend containing PBT, polymers functionalized with glycidyl methacrylate (GMA) have been often used as reactive compatibilizers.<sup>[7–11]</sup> Moreover, in some case, dual compatibilizers were used. Ju and Chang<sup>[4]</sup> investigated poly(ethylene terephthalate) (PET)/polystyrene (PS)/styrene-maleic anhydride copolymer (SMA) system. They found that the reaction between the anhydride group of SMA and the hydroxyl group of PET was unlikely to occur or occurred insignificantly. However, the combination of SMA and poly[methylene (phenylene isocyanate)] (PMPI) was demonstrated to be an effective dual compatibilizer for the PET/PS blend. The isocyanate group of PMPI reacted with both terminal groups of PET and the hydroxyl group of ring-opened

cible blend, suitable block or graft copolymers are added to the blend as a compatibilizer. In the industrial use, reactive processing is preferred, that is, addition of functionalized polymer, which is miscible with one blend component and reactive toward the other one, leads to the *in situ*-formed graft copolymer. The copolymer tends to stay at the interface, and thus acts as an effective compatibilizer between two immiscible polymers.<sup>[3–6]</sup>

Graduate School of Science and Engineering, Department of Organic and Polymeric Materials, Tokyo Institute of Technology, Ookayama, Meguro-ku, Tokyo 152-8552, Japan  
Fax: (+81) 3 5734 2423  
E-mail: tougizawa@o.cc.titech.ac.jp

SMA to form PET-PMPI-SMA copolymer during the melt blending. This copolymer acted as a compatibilizer and the compatibilized blends exhibited higher viscosity, finer phase domain, and improved mechanical properties.

Jun et al.<sup>[12]</sup> studied a blend of PBT with ethylene-propylene elastomer (EPM) grafted with isocyanate-containing monomer (HI). They found that there was chemical reaction between the isocyanate group of HI-grafted EPM and end groups of PBT, i.e. hydroxyl and carboxyl groups. The reactions resulted in both the finer blend morphology and the improvement of notched impact strength. Kim et al.<sup>[13]</sup> reported that both tensile strength and strain at break of HDPE/PET blend were improved by HDPE functionalized with blocked isocyanate group.

Under such a situation, Oyama et al.<sup>[14]</sup> reported the morphology of reactive blends of PBT/styrene-acrylonitrile random copolymer (SAN). They compared the morphology of PBT/SAN non-reactive blend with that of PBT/SAN-GMA reactive blend and then the latter showed finer dispersed particles than the former. Moreover, they added PMPI to PBT/SAN and found that the blend showed highly oriented co-continuous-like structures. Though it is expected that such the co-continuous-like structures would bring about a good mechanical property, there was no description about the property but only the morphology.

In this study, tensile properties of reactive PBT/SAN blends was investigated, where SAN was matrix component of ABS. Especially, the properties of PMPI added blend are focused and the relation between the tensile properties and the morphology is discussed.

## Experimentals

### Materials and Sample Preparation

PBT and SAN were supplied by BASF. The characteristics of the materials used in this work are shown in Table 1. SAN containing

**Table 1.**  
Materials characteristics

Name	Mn	Mw	Functionality ( $\mu\text{mol/g}$ )
PBT	10,200	45,800	[COOH] 13 [OH] 101
SAN	68,000	180,000	–
SAN-GMA	74,000	166,600	141

25 wt% of acrylonitrile (AN) without any functional groups and SAN-GMA random copolymer, that is, SAN functionalized with GMA (containing 23 wt% of AN and 2 wt% of GMA) were used. The reactive coupler, PMPI with 2.7 isocyanate groups per chain, was also obtained from BASF.

PBT, SAN and SAN-GMA were dried at 80 °C for at least 24 h before melt-mixing process. All melt blending was carried out at 250 °C for 9 min in a one-gram scale mixer, Mini-Max Molder (CS-183 MM, Custom Scientific Instruments Inc.). Immediately after the mixing, the blended samples were quenched in an ice water bath.

### Tensile Test

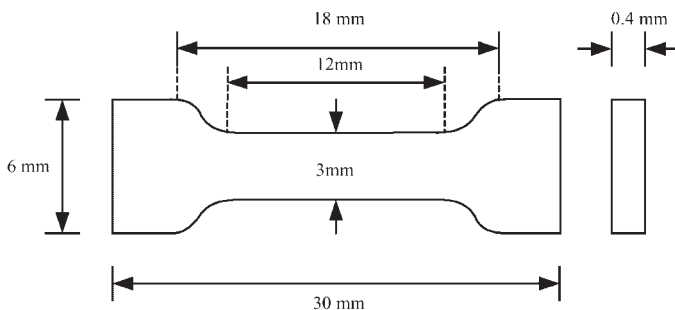
Tensile specimen was molded with a hot-pressing machine in dumbbell shape as shown in Figure 1. Tensile test was carried out with a tensile testing machine (Tensilon UTM-II-20, Toyo Baldwin Co.Ltd.) at room temperature with a crosshead speed of 2 mm/min. Tensile modulus, yield strength and strain at break were estimated from the measurement.

### Morphology Analysis

The blend specimen was microtomed to ultrathin sections of 70 nm thickness, using a Reichert-Nissei ULTRACT-N microtome with a diamond knife, and then they were stained with RuO<sub>4</sub> vapor. The morphology of the blend was observed by a transmission electron microscope (TEM), JEM 100CX (100kV).

### Measurement of Interfacial Adhesion

In order to measure interfacial adhesion, the interfacial fracture toughness ( $G_c$ ) of a

**Figure 1.**

Schematic representation of sample for the tensile test.

crack propagating at the interface between two polymers was measured by asymmetric double cantilever beam (ADCB) method for a strip-shaped sample, which was prepared by joining two polymer strips by annealing. This measurement determines the amount of energy released with a crack growth at an interface, and it provides a strength of interfacial adhesion.<sup>[15–20]</sup>

As a specimen for the fracture toughness measurement, PBT or PBT mixed with PMPI for 2 min at 250 °C was hot-pressed into a strip at 250 °C. SAN and SAN-GMA were also hot-pressed into a strip at 225 °C. SAN or SAN-GMA strip was placed on PBT or PBT/PMPI strip, and the two-layered samples were annealed at 250 °C for 15 min to form the adhesive bonding between the strips. As shown in Figure 2, a single-edged razor blade with thickness  $\Delta$  was manually inserted into the interface of the two-layered strip at the room temperature. After 50 h, the crack opening length between the edge of the blade and the crack tip was measured using an optical microscope with the help of x-y stage with an accuracy of 0.1 mm. This procedure was

repeated three times in one specimen, at least nine values of the crack length were obtained, and then the mean average value was calculated.

The fracture toughness ( $G_c$ ) was calculated by the following equation:<sup>[16]</sup>

$$G_c = \frac{3\Delta^2 E_1 h_1^3 E_2 h_2^3}{8a^4} \times \frac{E_1 h_1^3 C_2^2 + E_2 h_2^3 C_1^2}{[E_1 h_1^3 C_2^3 + E_2 h_2^3 C_1^3]^2} \quad (1)$$

$$C_1 = 1 + (0.64h_1/a)$$

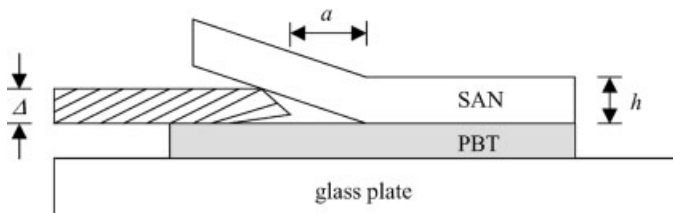
$$C_2 = 1 + (0.64h_2/a)$$

where the subscripts 1 and 2 stand for PBT and SAN, respectively. The  $E$ ,  $h$ ,  $a$  and  $\Delta$  represent the Young's modulus, the thickness of polymer strip, the crack length and the thickness of razor blade, respectively.

## Results and Discussion

### Tensile Property of PBT/SAN-GMA Blend

Figure 3 shows stress-strain curves for PBT/SAN-GMA (70/30) and PBT/SAN (70/30).

**Figure 2.**

Schematic representation of sample for the ADCB test.

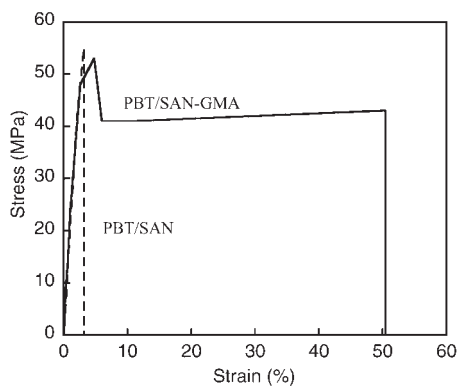


**Figure 3.** Stress-strain curves of the blends: dashed line = PBT/SAN (70/30) and solid line = PBT/SAN-GMA (70/30).

Each of the tensile modulus and the yield strengths took approximately the same values between the blends. However, PBT/SAN-GMA behaved in ductile manner, that is, it showed a yield point and the strain at break was 50%, while non-reactive PBT/SAN behaved in brittle manner, that is, it did not show necking and failed before the yielding and its strain at break was only 3%. Modification of SAN with 2% GMA group improved the ductility of PBT/SAN blend, though the tensile properties of neat SAN-GMA were the same as those of neat SAN. The TEM images of PBT/SAN (70/30), PBT/SAN-GMA (70/30) and the necking region of the latter after the tensile test are shown in Figure 4. The dark and bright regions in the TEM images correspond to PBT (more stained by  $\text{RuO}_4$ ) and SAN (less stained), respectively. Both PBT/

SAN and PBT/SAN-GMA blends showed ordinary sea-island morphology (Figures 4a and 4b), where PBT was matrix phase and SAN or SAN-GMA was dispersed phase. The particle size of dispersed phase in reactive PBT/SAN-GMA blend was finer than in non-reactive PBT/SAN blend. Moreover, the dispersed phase deformed to the tensile direction without void formation and then became ellipsoidal shape at the necking region (Figure 4c). These results imply that the reaction between PBT and SAN-GMA generated the PBT-SAN graft copolymer at the interface and the *in situ*-formed copolymer played a role of emulsifier to prevent the particle coalescence and to reduce the interfacial tension. When the PBT/SAN-GMA blend was annealed at 250 °C, which was the temperature above the melting temperatures of PBT and SAN-GMA, the morphology did not changed. The fact also confirms the copolymer formation at the interface. Martin et al.<sup>[8,21,22]</sup> has been investigating the reaction between PBT and epoxide-containing rubber in polymer blends. They reported that some reactions containing PBT-rubber copolymer formation took place between PBT and epoxide-containing rubber. In PBT/SAN-GMA blend, the similar reactions would also take place during melt-mixing process and then PBT-SAN copolymer would be formed. Though the reactions are complicated, the modification of SAN by GMA is effective for both reduction of particle size in PBT/SAN blend and improving the interfacial adhesion.

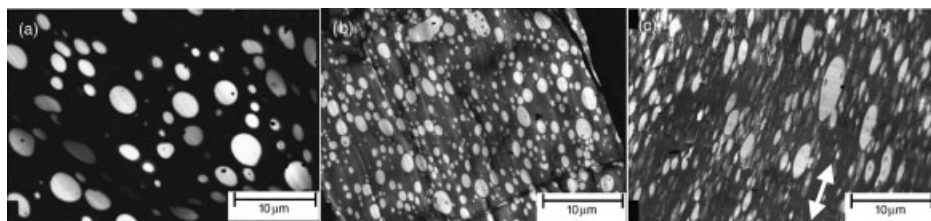


**Figure 4.** TEM micrographs of the blends: (a) PBT/SAN (70/30), (b) PBT/SAN-GMA (70/30) and (c) a necking region of the latter after the tensile test. The arrow indicates the tensile direction.

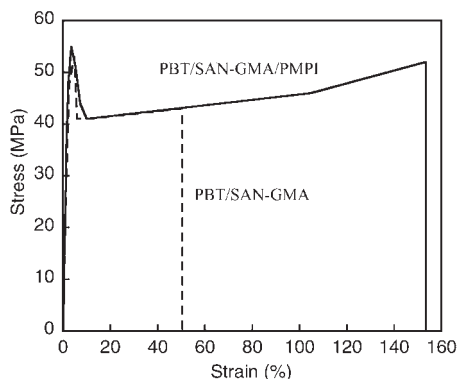


**Figure 5.**

Stress-Strain curves for the blends: dashed line = PBT/SAN-GMA (70/30) and solid line = PBT/SAN-GMA/PMPI (70/30/2) blends.

#### PMPI Effect in PBT/SAN-GMA Blend

PMPI can react with the end-groups of PBT and the epoxide group in SAN-GMA. Therefore, it was expected that the copolymerization between PBT and SAN-GMA would be assisted by addition of PMPI. Figure 5 is stress-strain curves of PBT/SAN-GMA/PMPI (70/30/2) and PBT/

SAN-GMA (70/30). The strain at break of PBT/SAN-GMA (70/30) took three times higher value by addition of PMPI (2 phr). TEM images of PBT/SAN-GMA/PMPI and the necking region by the tensile test are shown in Figure 6. The SAN dispersed phase in PBT/SAN/PMPI (Figure 6a) was both string-like domains and finer spherical particles, while that of PBT/SAN-GMA (Figure 4b) was approximately spherical shape, that is, the morphology of PBT/SAN-GMA blend was strongly affected by PMPI. The dispersed phase with not only the fine spherical particles but also even the string-like domains was strongly elongated to the tensile direction in the necking region (Figures 6b and 6b'). From the TEM images, it is considered that the improved strain at break in PBT/SAN-GMA/PMPI result from both such a longer elongated dispersed domain than that in PBT/SAN-GMA and the finer morphology. The strong elongation would result from the improvement of interfacial adhesion strength. Moreover, for the finer morphology, it

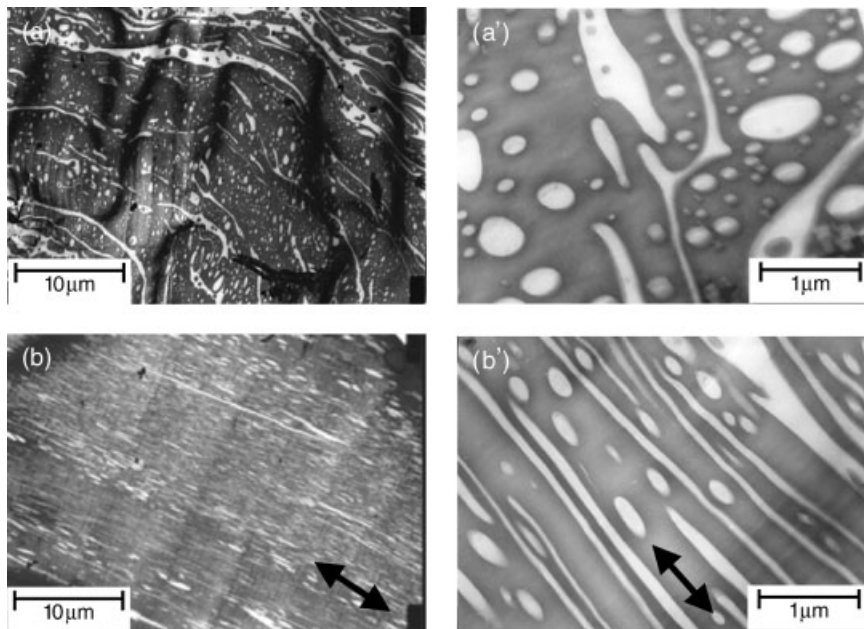


**Figure 6.**

TEM micrographs of PBT/SAN-GMA/PMPI (70/30/2) blend before tensile test ((a), (a')) and the necking region after the tensile test ((b), (b')). The arrows indicate the tensile direction.

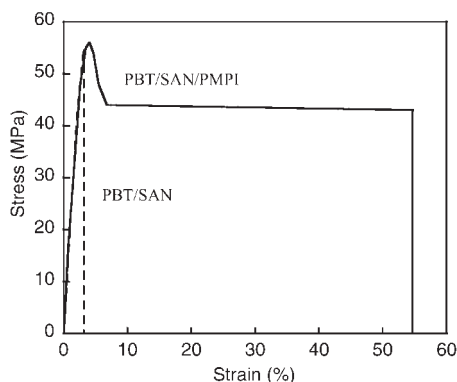


**Figure 7.**

Stress-Strain curves for the blends: dashed line = PBT/SAN (70/30) and solid line = PBT/SAN/PMPI (70/30/4) blends.

was reported that PMPI addition to PBT/SAN-GMA led to the finer dispersed phase by the viscosity effect and the facilitated pullout of copolymer chains from the interfacial region due to PBT chain extension by reaction with PMPI.<sup>[14]</sup>

#### PMPI Effect in PBT/SAN Blend

It was reported that PMPI addition was also effective for PBT/SAN blend to reduce the size of dispersed phase by viscosity effect.<sup>[14]</sup> Therefore, it was expected that tensile properties of PBT/SAN were also comparatively improved by addition of PMPI due to the finer morphology, though effect of compatibilizer (i.e. PBT-SAN copolymer) formation may not be expected.

Tensile test was carried out for PMPI added PBT/SAN (70/30) blend. When the amount of added PMPI was 2 phr, the blend behaved in brittle manner. However, it was found that PBT/SAN/PMPI (70/30/4) showed ductile behavior and yielded as shown in Figure 7, though PBT/SAN (70/30) failed in brittle manner prior to yielding.

In general, the principal factors, which affect the strain at break of a blend, are both the interfacial adhesion strength between matrix and dispersed phase and the size of dispersed phase, though there are many factors. Therefore, the interfacial

**Table 2.**

Molecular weight of SAN and SAN + PMPI.

Materials	$M_n$ (g/mol)	$M_w$ (g/mol)	$M_w/M_n$
SAN	$3.6 \times 10^5$	$5.2 \times 10^5$	1.44
SAN + PMPI 4 phr	$3.7 \times 10^5$	$5.1 \times 10^5$	1.38

adhesion between PBT and SAN should play an important role in the PBT/SAN/PMPI system. Strain at break has been used to evaluate the degree of compatibility in polymer blend,<sup>[13]</sup> because it is sensitive to adhesion strength between blend components. However, PMPI would react only with PBT and not with SAN in this system. It was confirmed by the viscosity measurement of melt-mixed SAN/PMPI, that is, the viscosity of SAN did not increase by addition of PMPI.<sup>[14]</sup> We also confirmed it by the other measurements. The molecular weight of SAN with and without PMPI was measured by a gel permeation chromatography and the results were shown in Table 2. The molecular weight of SAN showed almost no change by addition of PMPI. Moreover, the domain size of dispersed phase in the PBT/SAN/PMPI (70/30/4) became larger by the annealing at 250 °C, though PBT/SAN-GMA did not. Such a coarsening of the domain indicates that there is no copolymer formation in the interface between PBT and SAN and it also means that the interfacial adhesion strength in PBT/SAN/PMPI may be weak. To confirm it, the fracture toughness  $G_c$  of polymer pairs, PBT/SAN, (PBT+PMPI)/SAN, and PBT/SAN-GMA were measured by ADCB method (Table 3). The values of  $G_c$  in both PBT/SAN and (PBT+PMPI)/SAN were very low and took almost the same value. On the other hand, PBT/SAN-GMA showed extremely higher value than the

**Table 3.**

Fracture toughness of the interface between PBT (with or without PMPI) and SAN or SAN-GMA.

Samples	$G_c$ (J/m <sup>2</sup> )
PBT/SAN	25
(PBT + PMPI)/SAN	30
PBT/SAN-GMA	~2000



other samples. The results indicated that ductility in tensile property of the PBT/SAN/PMPI blend could not be explained by the improvement of interfacial adhesion.

The domain size of dispersed phase is also important factor for the tensile property. As described above, the fine morphology was obtained in PBT/SAN/PMPI blend just after melt-mixing process, however, the coarsening took place by the annealing at 250 °C. In our sample preparation, the dumbbell shaped specimen was molded by hot-pressing machine at 250 °C and it also brought about the coarsening. Therefore, the ductile behavior in PBT/SAN/PMPI resulted from neither the expected finer morphology nor the improved interfacial adhesion.

Figure 8 shows the TEM image of the necking region in PBT/SAN/PMPI (70/30/4) blend after the tensile test. The anomalous phenomenon, that is, the large SAN dispersed phase was largely elongated to the tensile direction without void formation was observed. It is known that the fine morphology or/and the good adhesion strength at the interface are needed to be elongated for the brittle dispersed phase. However, the PBT/SAN/PMPI blend did not satisfy the either requirement.

The plastic deformation of brittle dispersed phase in ductile matrix was reported by some researchers. Kurauchi and

Ohta,<sup>[23]</sup> and Koo et al.<sup>[24]</sup> reported that polycarbonate blends with ABS or SAN exhibited ductile fracture in the limited composition and showed elongation in the tensile test even though SAN was a typical brittle material. Kurauchi and Ohta<sup>[23]</sup> proposed that the SAN, which was normally brittle, underwent cold drawing which occurred owing to a compressive stress on the equatorial plane of the particles which transformed the deformation mode from crazing to shear yielding. From the studies on the pressure dependence of bulk deformation of brittle plastics, it is known that brittle plastics behave as if they were ductile under high pressure above a certain critical value.<sup>[25]</sup> For such a plastic deformation, von Mises's criterion is well known, which gives the condition for yielding:

$$(\sigma_x - \sigma_y)^2 + (\sigma_y - \sigma_z)^2 + (\sigma_z - \sigma_x)^2 \geq 6k^2 \quad (2)$$

where  $\sigma_x$ ,  $\sigma_y$  and  $\sigma_z$  are the three principal stresses, and  $k$  is a material constant. The physical meaning of Equation 2 is that yielding of material will take place when the shear strain energy density reaches a critical value. In order to fulfill the criterion in the blend, the dispersed phase must be in specific conditions, for example, finer morphology, strong adhesion strength at the interface between matrix and dispersed phase, high negative pressure application to the equatorial plane against the tensile direction, and so on. In the case of PBT/SAN/PMPI, it was confirmed that the former two conditions were not satisfied. Therefore, to fulfill the requirement of von Mises's criterion for yielding in PBT/SAN/PMPI, a mechanical property of the PBT or SAN should be changed by addition of PMPI. As described before, SAN did not react with PMPI, and the SAN/PMPI blend behaved in brittle manner. On the other hand, the reaction between PBT and PMPI brought about the chain extension and branching because of 2.7 isocyanate groups per PMPI chain.<sup>[14]</sup> Therefore, to confirm the effect of PMPI on PBT, the tensile test

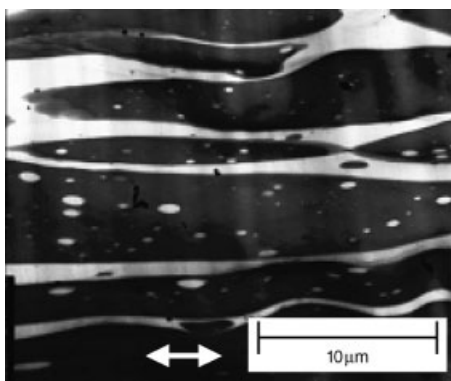


**Figure 8.**

TEM micrograph of PBT/SAN/PMPI (70/30/4) necking region near the fracture surface. The arrow indicates the tensile direction.

**Table 4.**

Tensile properties and crystallinity of PBT and PBT/PMPI.

Materials	Modulus (GPa)	Yield strength (MPa)	Strength at break (MPa)	Strain at break (%)	%Crystallinity of PBT (%)
PBT	1.7	57	49	276	34
PBT/PMPI 0.7 phr	1.8	52	44	242	32
PBT/PMPI 2 phr	1.8	51	50	232	27
PBT/PMPI 4 phr	1.6	50	50	241	22

was performed for PBT/PMPI, that is, the change of mechanical properties by PMPI addition was examined. Table 4 shows the tensile properties of PBT with different content of PMPI. Although neat PBT showed slightly higher value of strain at break rather than PBT/PMPI, every tensile property in PBT/PMPI was almost the same, each other, independent of the amount of added PMPI. It was expected that the crystallinity of PBT decreased with increasing reaction because of PBT chain extension and branching and indeed the values decreased with increasing the amount of added PMPI. From these results, since the effect of increasing of molecular weight on tensile properties is counter-balanced to the effect of decreasing crystallinity, it is considered that the tensile properties are independent of the amount of PMPI.

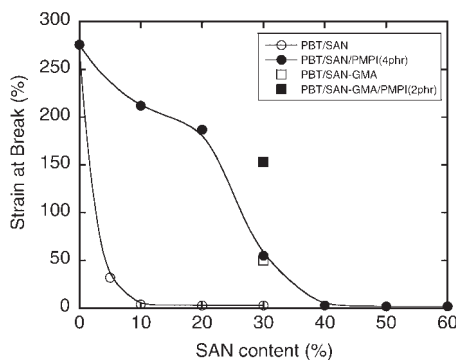
Although we could not find the difference between the tensile property of PBT and that of PBT/PMPI, it is suggested that there is another mechanism without both the fine morphology and the improvement of interfacial adhesion from the results described above. It is considered that the considerably ideal pressure, which satisfied the von Mises's criterion for yielding, would be applied to the SAN dispersed phase in PBT/SAN/PMPI blend and then the blend showed the ductile behavior.

#### Composition Dependence of the Blends on Tensile Property

As described above, only the composition of 70/30 in PBT/SAN system was examined. Here, the composition dependence of the properties in PBT/SAN/PMPI blend is discussed in order to understand the detail of this phenomenon.

Figure 9 shows the SAN content dependence of strain at break of PBT/SAN blends. Even PBT/SAN without PMPI showed ductile behavior when the composition of PBT/SAN was 95/5. As is clear from this result, even non-reactive PBT/SAN blend exhibited the ductile behavior when the SAN content was small. It can be considered that the phenomenon resulted from filling the requirement of von Mises's criterion for yielding by its finer morphology.<sup>[25]</sup> Moreover, it is clear that the transition from ductile to brittle took place at much larger SAN content in PBT/SAN/PMPI system than in PBT/SAN. The result suggests that PMPI has the function to shift the SAN content at the brittle-ductile transition in the blends to higher value. Namely, the effect of addition of PMPI makes the ductile region enlarge without reduction of other tensile properties.

The data of PBT/SAN-GMA (70/30) system are also plotted in this figure. Though composition dependence of tensile

**Figure 9.**

SAN content dependence of strain at break in PBT/SAN blends: ○ PBT/SAN, ● PBT/SAN/PMPI, □ PBT/SAN-GMA and ■ PBT/SAN-GMA/PMPI.



properties in these blends was not measured, the effect of PMPI must make the ductile region of SAN content in PBT/SAN-GMA blend enlarge as same as in PBT/SAN and shifted the curve to higher SAN content.

## Conclusions

Toughening of PBT/SAN blend was attempted by reactive blending. The tensile property was improved by reactive blending of PBT/SAN-GMA. PMPI addition to the blend further improved the tensile property and it was observed that the finer morphology was elongated during the tensile test. Such an elongation of brittle dispersed phase was also observed in PBT/SAN/PMPI blend. In the cases of PBT/SAN-GMA and PMPI added one, the interfacial adhesion strength was improved by PBT-SAN copolymer formation in the interface between PBT matrix and SAN dispersed phase. On the other hand, the interfacial adhesion strength was weak in PBT/SAN/PMPI because there was no reaction between SAN and PMPI or PBT. Moreover, it was observed by TEM that ductile behavior in PBT/SAN/PMPI might be due to the plastic deformation of the brittle particles and found that the string-like dispersed phase was largely elongated in the necking region. Though details of the mechanism are under consideration, the situation for toughening in PBT/SAN/PMPI is different from the ordinary compatibilized polymer blend, and then this may be a new approach to improve the mechanical property of the polymer blend.

In order to examine the details of this phenomenon, composition dependence of PBT/SAN/PMPI blends on ductility improvement were examined. From the comparison between values of strain at break in PBT/SAN with and without PMPI, it was found that PMPI addition made shift the strain at break vs. SAN content plot to larger SAN content region.

From this work, it is thought that PMPI worked as a kind of compatibilizer of PBT/SAN blend without copolymer formation at the interface. Moreover, we may not need to use ABS resin, which includes rubber, in order to improve the impact strength of PBT.

- [1] E. Hage, W. Hale, H. Keskkula and D.R. Paul, *Polymer* **1997**, 38, 3237.
- [2] W. Hale; L. A. Pessan, H. Keskkula and D.R. Paul, *Polymer* **1999**, 40, 4237.
- [3] H. Cartier, G.-H. Hu, *J. Mater. Sci.* **2000**, 35, 1985.
- [4] M.-Y. Ju, F.-C. Chang, *Polymer* **2000**, 41, 1719.
- [5] N. Kitayama, H. Keskkula, D.R. Paul, *Polymer* **2000**, 41, 8041.
- [6] P. Charoensirisomboon, T. Chiba, S.I. Solomko, T. Inoue, M. Weber, *Polymer* **1999**, 41, 6803.
- [7] H. Yang, M. Lai, W. Liu, C. Sun, J. Lie, *J. Appl. Polym. Sci.* **2002**, 85, 2600.
- [8] P. Martin, J. Devaux, R. Legras, M. van Gurp, M. van Duim, *Polymer* **2001**, 42, 2463.
- [9] W.R. Hale, L.A. Pessan, H. Keskkula, D.R. Pual, *Polymer* **1999**, 40, 4237.
- [10] D.S. Lee, J.K. Doo, B. Kim, J. Kim, *J. Polym. Eng.* **1998**, 18, 17.
- [11] C.-H. Tsai, F.-C. Chang, *J. Appl. Polym. Sci.* **1996**, 61, 321.
- [12] J.-B. Jun, J.-G. Park, D.-H. Kim, K.-D. Suh, *Eur. Polym. J.* **2001**, 37, 597.
- [13] D.-H. Kim, K.-Y. Park, J.-Y. Kim, K.-D. Suh, *J. Appl. Polym. Sci.* **2000**, 78, 1017.
- [14] H. T. Oyama, T. Kitagawa, T. Ougizawa, T. Inoue, M. Weber, *Polymer*, **2004**, 45, 1033.
- [15] E. Boucher, J.P. Folkers, H. Hervet, L. Le'ger, C. Creton, *Macromolecules* **1996**, 29, 774.
- [16] B. Bernard, H.R. Brown, C.J. Hawker, A.J. Kellock, T.P. Russel, *Macromolecules* **1999**, 32, 6254.
- [17] C. Creton, E.J. Kramer, C.-Y. Hui, H.R. Brown, *Macromolecules*, **1992**, 25, 3075.
- [18] E.A. Eastwood, M.D. Dadmun, *Macromolecules*, **2002**, 35, 5069.
- [19] E.A. Eastwood, M.D. Dadmun, *Polymer* **2002**, 43, 6707.
- [20] C.-A. Dai, K.D. Jandt, D.R. Iyengar, N.L. Slack, K.H. Dai, W.B. Davidson, E.J. Kramer, C.-Y. Hui, *Macromolecules* **1997**, 30, 549.
- [21] P. Martin, C. Gallez, J. Devaux, R. Legras, L. Leemans, M. van Gurp, M. van Duim, *Polymer* **2003**, 44, 5251.
- [22] P. Martin, J. Devaux, R. Legras, L. Leemans, M. van Gurp, M. van Duim, *J. Appl. Polym. Sci.*, **2004**, 91, 703.
- [23] T. Kurauchi, T. Ohta, *J. Mater. Sci.*, **1984**, 19, 1699.
- [24] K.-K. Koo, T. Inoue, K. Miyasaka, *Polym. Eng. Sci.*, **1985**, 25, 741.
- [25] K. Matsushige, S.V. Radeliffe, E. Baer, *J. Appl. Polym. Sci.*, **1976**, 20, 1853.